ELSEVIER

Polymer 40 (1999) 3781–3786

polymer

Solid-state ^{13}C-NMR analyses of the structure and chain conformation of thermotropic liquid crystalline polyether crystallized from the melt through the liquid crystalline state

Hiroyuki Ishida, Fumitaka Horii*

Institute for Chemical Research, Kyoto University Uji, Kyoto 611-0011, Japan

Received 24 June 1998; received in revised form 14 August 1998; accepted 24 August 1998

Abstract

Solid-state ^{13}C-NMR analyses of the structure and chain conformation have been carried out for a main-chain thermotropic liquid crystalline polyether which was polymerized with 4,4′-dihydroxy-α-methylstilbene and 1,9-dibromononane. This sample was crystallized by cooling from the isotropic melt through the nematic liquid crystalline state. Differential scanning calorimetry measurements and polarizing optical microscopic observation have confirmed that the nematic liquid crystalline phase clearly exists in the wide range of temperature in both heating and cooling scans. T_{1C} analyses have revealed that each resonance line of the methylene sequence contains three components with different T_{1C} values and these values become significantly longer with decreasing temperature. The evaluation of ^{13}C chemical shifts considering the γ-*gauche* effect indicates that methylene sequences for the two components with the longer T_{1C} values adopt the specific overall conformation, in which successive *trans-gauche* exchange and isolated *trans* conformations coexist. In contrast, all the C–C bonds of the methylene sequence for the component with the shortest T_{1C} value, which corresponds to the supercooled liquid crystalline component, is in the rapid *trans-gauche* exchange conformation, reflecting the conformation in the liquid crystalline state.

Keywords: CP/MAS ^{13}C NMR; Liquid crystalline polymers; Polyether

1. Introduction

In a previous paper [1], we reported the solid-state ^{13}C-NMR analysis of the structure and chain conformation for the thermotropic liquid crystalline polyurethane (PDBDM) which was built up from 3,3′-dimethyl-4,4′-biphenyldiyl diisocyanate, 1,10-decanediol and 1-hexanol. The analytical method used in that work has recently been developed to characterize the crystalline–noncrystalline structure and hydrogen bonding as well as molecular motion for different solid polymers such as polyolefins [2–7], polyether [8], polyesters [9,10], polyurethane [11], poly(vinyl alcohol) [12–14], cellulose [15–17], and so on. The detailed characterization of the PDBDM sample crystallized by cooling from the isotropic melt through the nematic liquid crystalline state led to the following results. T_{1C} analyses revealed that the sample contains three components with different T_{1C} values, which are ascribed to the crystalline, medium, and noncrystalline components. From the line shape analyses of these three components, the spacer methylene sequence composed of ten carbon atoms was found to be in the planar zigzag conformation for both crystalline and medium components. In contrast, the methylene sequence for the noncrystalline component, which corresponds to the supercooled liquid crystalline component, was found to be in the characteristic conformation, namely the alternate *trans* and *trans-gauche* exchange conformation, probably reflecting the conformation existing in the liquid crystalline state. Several publications also reported the characterization of the chain conformation and molecular motion in main-chain thermotropic liquid crystalline polymers by using solid-state ^{13}C-NMR spectroscopy, although the detailed component analysis was not carried out even in the solid state [18–20].

In this paper, we apply the same ^{13}C-NMR analysis as used in our previous paper [1] to the characterization of the structure and chain conformation for a main-chain thermotropic liquid crystalline polyether, which is synthesized with 4,4′-dihydroxy-α-methylstilbene and 1,9-dibromononane. The thermal properties, diffusion, and melt viscosity of this polymer have already been reported [21–24]. The sample, which is crystallized from the isotropic melt

* Corresponding author.

0032-3861/99/$ - see front matter
PII: S0032-3861(98)00610-7

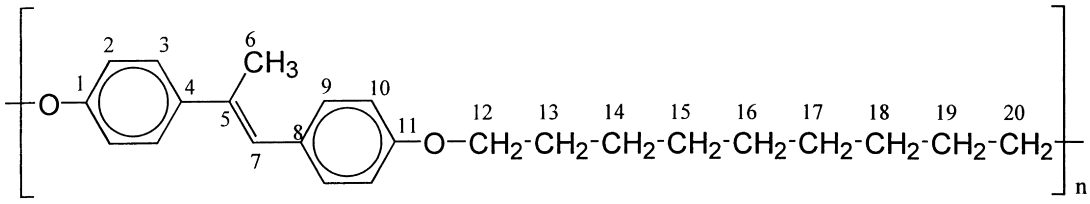

Scheme 1.

through the nematic liquid crystalline phase, is characterized as follows. First, resonance lines of the spacer methylene carbons in cross-polarization/magic angle spinning (CP/MAS) ^{13}C-NMR spectra are resolved into the contributions from different components on the basis of the difference in ^{13}C spin-lattice relaxation time. Next, the chain conformation of the methylene sequence is evaluated in detail for each component by considering the *γ-gauche* effect on the chemical shifts of methylene carbons. Moreover, the same analysis is carried out in the liquid crystalline state to clarify the conformation of the methylene sequence.

2. Experimental

2.1. Samples

The polyether sample (HMS-9), which was provided by Prof. J.S. Higgins of Imperial College, was synthesized with 4,4′-dihydroxy-α-methylstilbene as mesogen and 1,9-dibromononane as spacer. The chemical structure of HMS-9 is shown in Scheme 1. The number-average and weight-average molecular weights, which were determined by size exclusion chromatography with light scattering, were 1620 and 6280, respectively. This sample was crystallized under an argon atmosphere by cooling from 140°C, which corresponds to the isotropic phase, through the nematic liquid crystalline state at a rate of 0.4°C min^{-1}.

2.2. Solid-state ^{13}C-NMR measurements

Solid-state ^{13}C-NMR measurements were performed at −88 to 97°C on a JEOL JNM-GSX200 spectrometer equipped with a variable temperature MAS system operating at 50.05 MHz under a static magnetic field of 4.7 T. The sample was packed in a 7 mm cylindrical MAS rotor. In the case of measurements at 97°C, we used a MAS rotor with an O-ring seal [12–14] so that the sample did not leak from the rotor under a high centrifugal field. ^{1}H and ^{13}C radio-frequency field strengths $\gamma B_1/2\pi$ were 61.0–62.5 kHz. The contact time for the CP process was 2.0 ms and the recycle time after the acquisition of a flame ionization detector was 5 s throughout this work. The MAS rate was set to 3.6 kHz to avoid the overlapping of spinning side bands on other resonance lines. The number of scans was usually 400. ^{13}C chemical shifts were expressed as values relative to tetramethylsilane (Me_4Si) by using the CH_3 line at 17.36 ppm of hexamethyl benzene crystals as an external reference. ^{13}C spin-lattice relaxation times (T_{1C}) were measured by using the CPT1 pulse sequence [25].

2.3. Differential scanning calorimetry

Thermal transition behavior was measured by a TA Instruments DSC 2910 differential scanning calorimeter. Indium was used as a standard for temperature calibration. All differential scanning calorimetry (DSC) runs were made for 5.0 mg samples under a nitrogen atmosphere with different heating or cooling rates. First-order transitions were read as maxima or minima of the endothermic or exothermic peaks.

2.4. Optical microscopy

Thermal phase transitions and texture changes were observed with a Nikon OPTIPHOT2-POL optical polarizing microscope equipped with a Linkam LK-600PM hot stage. Powder-like HMS-9 was placed on a glass slide and covered with a glass cover slip. Each sample was heated or cooled under a nitrogen atmosphere in the hot stage at a fixed rate.

3. Results and discussion

3.1. Thermal transition behavior

In order to confirm the existence of the liquid crystalline phase for the HMS-9 sample, DSC measurements and polarizing optical microscopic observations have been performed. Fig. 1 shows DSC heating and cooling thermograms for the HMS-9 sample crystallized at a cooling rate of 0.4°C min^{-1}. On the cooling process at 10°C min^{-1}, one very small and broad exothermic peak at 96.6°C and one strong exothermic peak at 58.9°C appear as shown in Fig. 1(a). On the heating process at 10°C min^{-1}, two exothermic peaks clearly appear at 85.5°C and 110.5°C as shown in Fig. 1(b). Furthermore, polarizing optical microscopic observations have confirmed that the nematic liquid crystalline phase really forms in the temperature region between the two DSC peaks on both cooling and heating processes. Fig. 2 shows the typical mesomorphic texture appearing on the cooling process. Such thermal transition behavior is in good accord with the result previously reported [21].

3.2. CP/MAS ^{13}C-NMR spectrum

Fig. 3 shows the CP/MAS ^{13}C-NMR spectrum of the

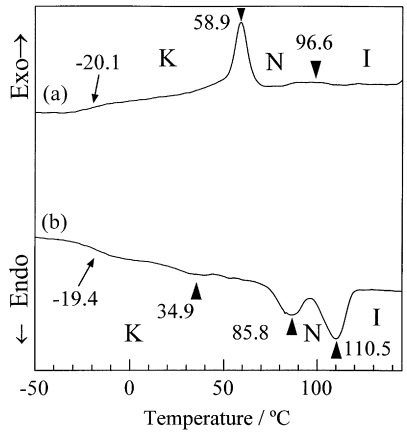

Fig. 1. DSC thermograms of HMS-9: (a) first cooling at 10°C min^{-1}; (b) second heating at 10°C min^{-1}. K, N and I indicate the crystalline, nematic liquid crystalline and isotropic phases, respectively.

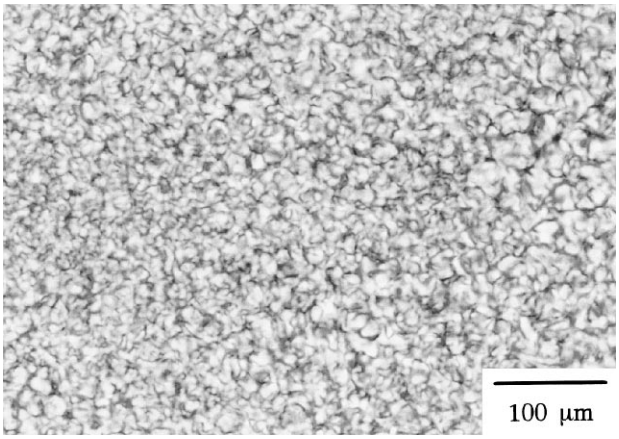

Fig. 2. Polarizing optical microphotograph for HMS-9 on cooling at 5°C min^{-1}.

HMS-9 sample measured at 43°C. The assignment of each resonance line has been made on the basis of the result for the solution-state spectrum measured at room temperature in $CDCl_3$. As is clearly seen in Fig. 3, resonance lines ascribed to the mesogen aromatic carbons and spacer methylene carbons are well separated from each other. However, the crystalline and noncrystalline contributions are not straightforwardly observed as differences in chemical shift like the case of PDBDM [1].

3.3. ^{13}C spin-lattice relaxation behavior

In order to examine the crystalline–noncrystalline structure of HMS-9, ^{13}C spin-lattice relaxation behavior has been measured at 43°C by the CPT1 pulse sequence [25].

In Fig. 4, the logarithmic peak intensity of the C13, C15, C16, C17, C19 methylene carbons is plotted against the decay time τ for the T_{1C} relaxation. Since the decay curve appears not to be a single exponential, it has been analyzed in terms of multiple components having different T_{1C} values by the computer-aided nonlinear least-squares method. The solid line is the composite curve calculated by assuming three components with different T_{1C} values, where the exponential decay of each component is also shown as a broken line. The experimental points agree well with the calculated curve, in the only case that there are three components with different T_{1C} values for the C13, C15, C16, C17, C19 lines. Interestingly, even the longest T_{1C} value is as short as 2.89 s, suggesting the enhanced molecular mobility in these three components. The resonance line of C14, C18 methylene carbons has also been found to contain three components with T_{1C} values of the order similar to those for the C13, C15, C16, C17, C19 lines. These three components are hereafter referred to as component I, component II, and component III in the order of decreasing T_{1C} value. In contrast, the mesogen carbons have been found to contain two components with different T_{1C} values, 5–9 s and 40–60 s, although these two components cannot be well correlated with the three components for methylene carbons at present. Nevertheless, the level of the longer T_{1C} values indicates much more restricted molecular mobility of the mesogen groups compared to the methylene sequence at room temperature.

3.4. Spectra of the three components

Fig. 5 shows ^{13}C-NMR spectra of the three components for the methylene carbons except for C12, C20 carbons, which were separately recorded by using the difference in T_{1C} as follows. The spectrum of component I was selectively measured using the CPT1 pulse sequence [25] by setting the T_{1C} decay time τ to 2.0 s. The spectrum of component II was obtained by subtracting the spectrum of component I from the spectrum measured with the CPT1 pulse sequence by setting $\tau = 0.5$ s. In these spectra, component III completely disappears due to the shorter T_{1C} values. As for component

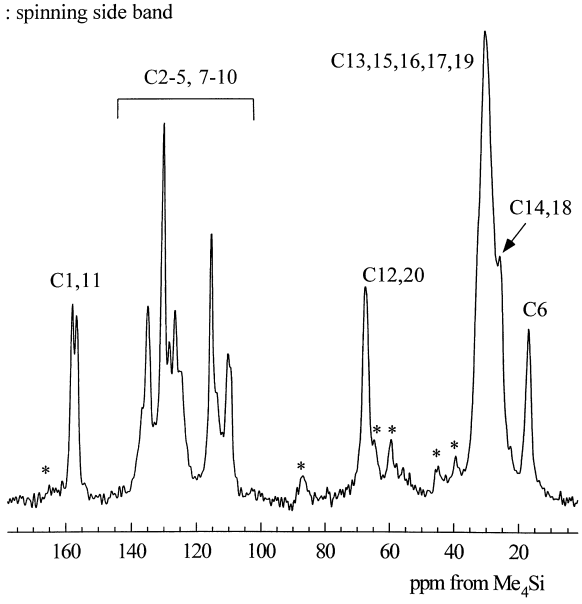

Fig. 3. 50 MHz CP/MAS ^{13}C-NMR spectrum of HMS-9 measured at 43°C.

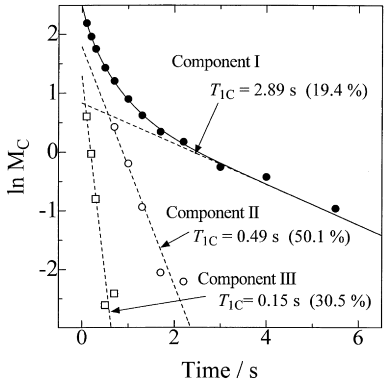

Fig. 4. ^{13}C spin–lattice relaxation process for the C13, C15, C16, C17, C19 methylene carbons measured by the CPT1 pulse sequence at 43°C.

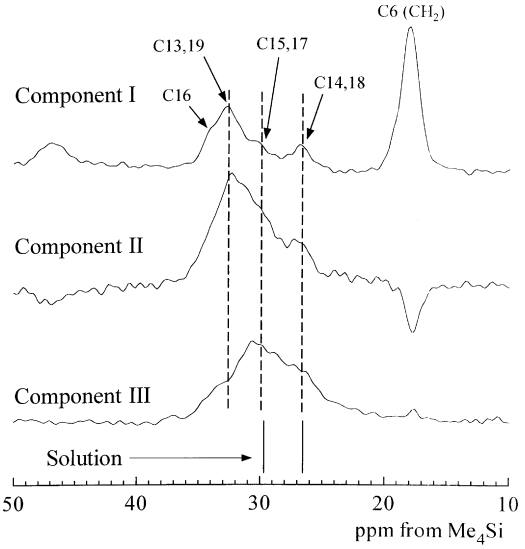

Fig. 5. ^{13}C-NMR spectra of different components of HMS-9: (a) component I; (b) component II; (c) component III.

III, the spectrum was measured by the saturation recovery method [2,8] modified for solid-state measurements by setting the T_{1C} recovery delay time to 0.1 s, although some minor contribution from component II is included in this spectrum.

In order to evaluate methylene sequence conformations for the three components, we intend to analyze the chemical shifts of the respective lines considering the *γ-gauche* effect [26]. The *γ-gauche* effect is the conformational effect on ^{13}C chemical shifts of the successive C–C–C–X sequence. In the case of the methylene sequence C^0–C^α–C^β–C^γ, carbon C^0 and its γ-substituent methylene carbon C^γ are separated by three intervening bonds, and their mutual distance and orientation are variable depending on the conformation of the central bond C^α–C^β. Therefore, the change in the conformation of the C^α–C^β bond brings about the variation in the electron shielding of C^0 by C^γ; the *gauche* conformation in the bond induces about a 5 ppm upfield shift for the C^0 carbon compared to the *trans* conformation.

First, we evaluate the methylene conformations of component I. The resonance lines for the C13, C15, C16, C17, C19 carbons, which appear at 35–28 ppm, seem to consist of three lines at about 34 ppm, 32.7 ppm, and 30 ppm. The differences in the chemical shifts for the three lines should be interpreted by the *γ-gauche* effect for the associated bonds. However, the *γ-gauche* effect in these cases must be reduced by rapid exchanges between the *trans* and *gauche* conformations, because the differences in chemical shifts are significantly smaller compared to the value (about 5 ppm) expected by the conventional *γ-gauche* effect. When the line appearing as a shoulder at about 34 ppm is assumed to be assigned to the methylene carbon having no *γ-gauche* effect, the lines at about 32.7 ppm and 30 ppm may be ascribed to the carbons which undergo the *γ-gauche* effect from the one and both side(s) of the methylene sequence, respectively. The comparison of the spectrum in Fig. 5 with the solution-state spectrum measured at room temperature in $CDCl_3$ for HMS-9 has confirmed that the most upfield line at about 30 ppm is almost in accord with the single line assignable to C13, C15, C16, C17, and C19 carbons in chemical shift. In the solution state, all the bonds in the methylene sequence should be in the rapid *trans-gauche* exchange conformation and then each methylene carbon may be subjected to the *γ-gauche* effect from both sides in the methylene sequence. Therefore, such an experimental accordance seems to support the interpretation made above for the line splitting of the methylene carbons for component I in terms of the *γ-gauche* effect. The chemical shifts for C12, C20 and C14, C18 carbons are also in good accord with their values for the solution-state spectrum. This accordance indicates that the chemical shifts of these lines should be interpreted in terms of the *γ-gauche* effect considering the rapid *trans-gauche* exchanges like the case in the solution state. Therefore, the C13–C14 bond for the C12 carbon, the C12–C13 and C15–C16 bonds for the C14 carbon, the C16–C17 and C19–C20 bonds for the C18 carbon, and the C18–C19 bond for the C20 carbon should be in the rapid *trans-gauche* exchange conformation. Since the four bonds C13–C14, C15–C16, C16–C17, and C18–C19 contain the *gauche* conformation, C15 and C17 carbons are affected doubly by the *γ-gauche* effect from both sides. Therefore, the small line observed at about 30 ppm should be assigned to C15, C17 carbons. In contrast, by considering the association of the lines at about 32.7 ppm and 34 ppm with the *γ-gauche* effect, it is reasonably found that the bonds C14–C15 and C17–C18 are in the *trans* conformation. Moreover, the lines at about 32.7 and 34 ppm should be assigned to the C13, C19 and C16 carbons, respectively. According to these assignments, the most probable conformations for the methylene sequence in component I are illustrated in Fig. 6(a).

As for component II, the chemical shifts of the respective lines are in good accord with those of component I in the methylene sequence. This fact indicates that component I

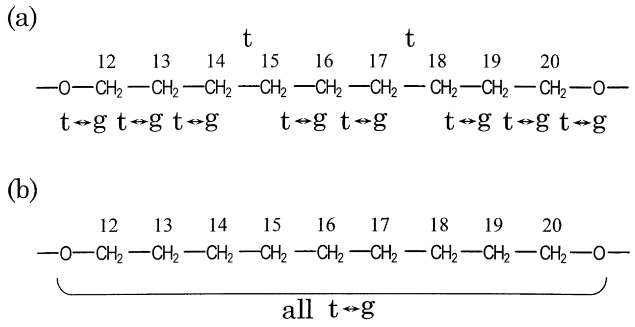

Fig. 6. Conformations for the methylene sequences in different components in HMS-9: (a) component I and component II; (b) component III.

has the same chain conformation as that for component I in the methylene sequence. Here, the relative intensities of the respective lines shown in Fig. 5 are not exactly proportional to the compositions of the respective carbons due to the difference in T_{1C} values. For component III, in contrast, the C13, C16, C19 resonance lines significantly shift upfield compared to the corresponding lines of components I and II. Moreover, the chemical shifts of the lines are in good accordance with the values of the corresponding solution-state spectrum. This result indicates that all the bonds of the methylene sequence for component III is in the rapid *trans-gauche* exchange conformation as shown in Fig. 6(b), possibly like in the solution-state.

3.5. CP/MAS ^{13}C-NMR measurements at various temperatures

To obtain further information of the spacer conformation, CP/MAS ^{13}C-NMR measurements were performed at -88 to 97°C. Fig. 7 shows the CP/MAS ^{13}C-NMR spectra of HMS-9 at various temperatures, which contain the contributions from components I–III described. With decreasing temperature, the resonance lines for C13, C15, C16, C17, C19 carbons are found to significantly shift downfield, whereas the chemical shifts for C12, C20 and C14, C18 carbons remain unchanged. Since T_{1C} measurements confirmed that there is no large change in the mole fraction of each component, such downfield shifts will not be due to the decrease in fraction of component III, but due to the change in conformation of this component. Namely, at low temperatures, the *trans-gauche* exchange conformation for the C14–C15 and C17–C18 bonds will be fixed to the *trans* conformation like the cases of components I and II. Since this change in conformation with temperature has been found to be a reversible process, some orientational factor of the mesogen group and the ether bond may prevent the fixation of the *trans* conformation in those bonds for component III, unlike the cases of components I and II.

Moreover, we have carried out similar ^{13}C-NMR analyses at 97°C which corresponds to the nematic liquid crystalline state. The molecular orientation induced under a static magnetic field B_0 may be randomized by MAS at 3.6 kHz.

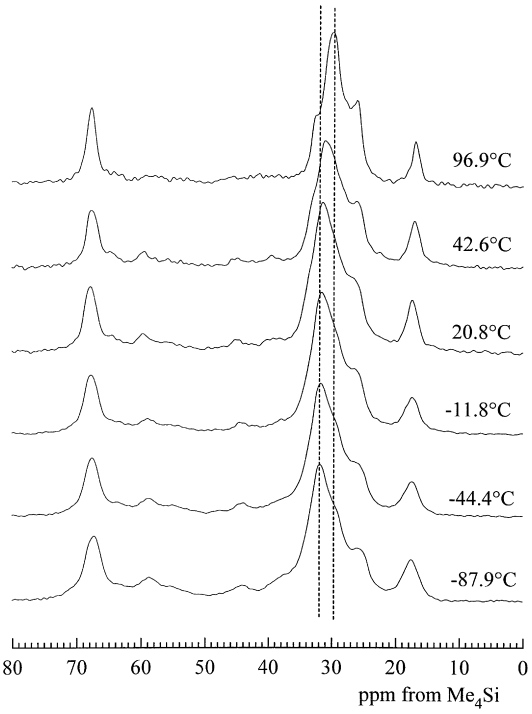

Fig. 7. 50 MHz CP/MAS ^{13}C-NMR spectra of HMS-9 measured at various temperatures.

In order to examine the structure in the liquid crystalline state, ^{13}C spin-lattice relaxation behavior has been measured at 97°C by the CPT1 pulse sequence [25]. In Fig. 8, the logarithmic peak intensity of the resonance line for the C13, C15, C16, C17, C19 methylene carbons is plotted against the decay time τ for the T_{1C} relaxation. The decay curve appears to be a single exponential and the T_{1C} value is determined as 0.50 s for this resonance line by the computer-aided least-squares method. The resonance line of C14, C18 methylene carbons was also found to have a single component with T_{1C} value of 0.40 s. In contrast, the resonance lines assignable to the mesogen carbons were found to contain two components with T_{1C} values of 24–61 s and 0.2–9.5 s, which are almost of the same order as those measured at 43°C. This indicates that the mesogen groups still undergo highly restricted molecular motion even in the liquid crystalline state.

The chemical shifts of the respective methylene carbons at 97°C are in good accordance with the values for component III at 43°C, indicating that in the nematic liquid crystalline state all C–C bonds of the methylene sequence in HMS-9 undergo the rapid *trans-gauche* exchanges similarly to the case for component III at 43°C. Accordingly, component III should be assigned to the supercooled liquid crystalline component. Cheng et al. also examined the conformation of the methylene spacer for a liquid crystalline polyether, MBPE-9, in the liquid crystalline state by solid-state ^{13}C-NMR spectroscopy [18]. Their finding for the conformation in the liquid crystalline state is in good accord with our result for components I and II in the solid state. In contrast,

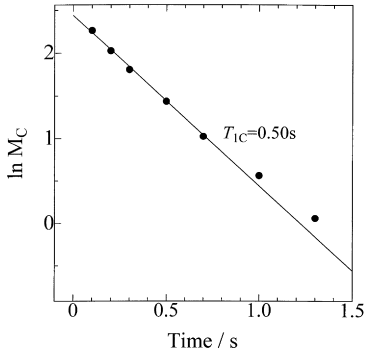

Fig. 8. ^{13}C spin-lattice relaxation process for the C13, C15, C16, C17, C19 methylene carbon measured by the CPT1 pulse sequence at 97°C.

the methylene sequence for our sample is in the rapid *trans-gauche* exchange conformation in the liquid crystalline state. Such a difference in conformation in the liquid crystalline state may be due to the structural difference in the mesogen groups.

More detailed characterization will be performed for a liquid crystalline polyether newly synthesized with 3,3′-dimethyl-4,4-dihydroxybiphenyl and α,ω-dibromoalkane.

Finally, it should be necessary to discuss the assignment of components I and II. A previous study [21] confirmed that HMS-9 has the crystalline phase below about 80°C. Since the prominent phase transition can be also observed in the corresponding temperature region for our sample as shown in Fig. 1, component I should be assigned to the crystalline component. Nevertheless, it should be noted that the methylene sequence of this component has extraordinarily high molecular mobility as a crystalline component as suggested by the short T_{1C} value. As for component II, the assignment is not yet established as is the case of PDBDM [1]. The component seems to be a metastable component that exists as a precursor before the crystallization.

4. Conclusion

The structure and chain conformation of the spacer methylene sequence for HMS-9 polyether have been characterized by solid-state ^{13}C-NMR analyses and the following conclusions have been obtained.

1. ^{13}C spin-lattice relaxation time (T_{1C}) analyses have revealed that there exist three components with different T_{1C} values for the spacer methylene chain in the solid state at 43°C. These components are referred to as components I, II, and III in the order of decreasing T_{1C}.
2. The interpretation of ^{13}C chemical shifts in terms of the *γ-gauche* effect has been performed to clarify the methylene sequence conformation for the three components. For component III with the shortest T_{1C} value, all the C–C bonds of the methylene sequence are in the rapid *trans-gauche* exchange conformation, reflecting the same conformation in the nematic liquid crystalline state. Therefore, component III should be assigned to the supercooled liquid crystalline component.
3. For components I and II, the methylene sequences are in somewhat ordered chain conformation, because two isolated *trans* conformations are introduced to successive *trans-gauche* exchange conformations at the definite position. Component I should be assigned to the crystalline component, whereas component II may be a metastable component existing as a precursor prior to the crystallization.

Acknowledgements

We thank Professor J.S. Higgins of Imperial College for kindly providing the main-chain liquid crystalline polyether HMS-9.

References

[1] Ishida H, Kaji H, Horii F. Macromolecules 1997;30:5799.
[2] Kitamaru R, Horri F, Murayama K. Macromolecules 1986;19:639.
[3] Saito S, Moteki Y, Nakagawa M, Horii F, Kitamaru R. Macromolecules 1990;23:3257.
[4] Kimura T, Neki K, Tamura N, Horii F, Nakagawa M, Odani H. Polymer 1992;33:493.
[5] Kitamaru R, Horii F, Zhu Q, Bassett DC, Olley RH. Polymer 1994;35:1171.
[6] Kuwabara K, Kaji H, Horii F, Bassett DC, Olley RH. Macromolecules 1997;30:7516.
[7] Horii F, Kaji H, Ishida H, Kuwabara K, Masuda K, Tai T. J Mol Struct 1998;441:303.
[8] Hirai A, Horii F, Kitamaru R, Fatou JG, Bello A. Macromolecules 1990;23:2913.
[9] Tsuji H, Horii F, Nakagawa M, Ikada Y, Odani H, Kitamaru R. Macromolecules 1992;25:4114.
[10] Kaji H, Horii F. Macromolecules 1997;30:5791.
[11] Ishida M, Yoshinaga K, Horii F. Macromolecules 1996;29:8824.
[12] Horii F, Hu S, Ito T, Odani H, Matsuzawa S, Yamaura K. Polymer 1992;33:2299.
[13] Hu S, Tsuji M, Horii F. Polymer 1994;35:2516.
[14] Horii F, Masuda K, Kaji H. Macromolecules 1997;30:2519.
[15] Yamamoto H, Horii F. Macromolecules 1993;26:1313.
[16] Yamamoto H, Horii F. Cellulose 1994;1:57.
[17] Yamamoto H, Horii F, Hirai A. Cellulose 1996;3:229.
[18] Cheng J, Jin Y, Wunderlich B, Cheng SZD, Yandrasits MA, Zhang A, Percec V. Macromolecules 1992;25:5991.
[19] Cheng J, Jin Y, Chen W, Wunderlich B, Jonsson H, Hult A, Gedde UW, J Polym Sci Part B: Polym Phys 1994;32:721.
[20] Cheng J, Yoon Y, Ho R-M, Leland M, Guo M, Cheng SZD, Chu P, Percec V. Macromolecules 1997;30:4694.
[21] Percec V, Nava H. J Polym Sci Part A: Polym Phys 1987;25:405.
[22] Percec V, Asami K, Tomazos D, Feijoo JL, Unger G, Keller A. Mol Cryst Liq Cryst 1991;205:47.
[23] Percec V, Asami K, Tomazos D, Feijoo JL, Unger G, Keller A. Mol Cryst Liq Cryst 1991;205:67.
[24] Hall E, Ober CK, Kramer EJ, Colby RH, Gillmor JR. Macromolecules 1993;26:3764.
[25] Torchia DA. J Magn Reson 1981;44:117.
[26] Tonelli AE, NMR Spectroscopy and Polymer Microstructure: The Conformational Connection. New York: VCH, 1989.